Time-dependent studies of single and multiple photoionization of H_2^+

J. Colgan, M. S. Pindzola, and F. Robicheaux
Department of Physics, Auburn University, Auburn, Alabama 36849, USA
(Received 30 June 2003; published 22 December 2003)

A time-dependent method is used to study the photoionization of the simplest one-electron molecule, H_2^+. We use the variational principle to solve the time-dependent Schrödinger equation for H_2^+ in spherical coordinates (r,θ) centered on the center of mass of the H_2^+ system in a time-varying electromagnetic field, in the fixed-nuclei approximation. Bound and continuum states of H_2^+ are obtained by diagonalizing the two-dimensional Hamiltonian for H_2^+ on a uniform lattice. Two different algorithms for the time propagation of the Schrödinger equation are described, the first an explicit time propagator involving matrix multiplication and the second an implicit time propagator involving matrix inversion. Single-photoionization cross sections for H_2^+ are presented for the cases where the laser field is oriented both parallel and perpendicular to the internuclear axis. Excellent agreement is found between the present calculations and previous work. Two- and three-photon ionization cross sections are also presented for the cases where the laser field is oriented both parallel and perpendicular to the internuclear axis. Comparison with previous work is available only for the parallel orientation case where good agreement is found with a previous time-independent calculation.

DOI: 10.1103/PhysRevA.68.063413 PACS number(s): 33.80.Rv

I. INTRODUCTION

The study of the simplest one-electron molecule, H_2^+, has attracted much attention from both theory and experiment in recent years. The advent of increasingly powerful laser sources has intensified the study of laser-matter interactions so that now femtosecond (or even subfemtosecond) pulses are almost routine. Molecular targets can be much more interesting than their atomic counterparts due to the rich variety of physical processes which can be observed only in molecules, for example, bond softening (hardening), above-threshold dissociation, vibrational excitation, Coulomb explosions, and the competition between dissociation and ionization. Earlier work in these areas has been extensively discussed and reviewed [1]. Of course, these physical phenomena inevitably require a much more complex theoretical description of the processes involved. Although the one-electron H_2^+ system can be solved exactly in elliptical coordinates [2], the full solution of a one-electron molecule subjected to an intense electromagnetic field is still a formidable task.

In recent years many theoretical groups have performed numerical calculations of the dynamical processes undergone by H_2^+ in the presence of an intense electromagnetic field. It is common practice to make severe approximations to the full dimensionality of the problem to make it computationally tractable. This can involve restricting the electron coordinate to one dimension, or freezing the nuclear motion (the Born-Oppenheimer approximation) during which the electrons move in the field of the ''frozen'' nuclei. For example, Bandrauk and co-workers have made many time-dependent calculations on photoemission spectra from and the dissociative ionization of H_2^+ (Refs. [3,4], and references within). In recent years they have focused on H_2^+ under the influence of ultrashort (attosecond) pulses [5] and the effect on high-order harmonic generation. Recent three-dimensional numerical solutions of the time-dependent Schrödinger equation for H_2^+ have also been obtained by Dundas *et al.* [6] in the fixed-nuclei approximation. Very recently time-dependent model calculations of H_2^+ in an ultrashort laser pulse have been made by Ver Steeg *et al.* [7], who restricted the electronic motion to one dimension while allowing the nuclei to move along a second dimension. Similar reduced-dimensionality calculations have also been made by Feuerstein and Thumm [8], who studied fragmentation parameters as a function of the initial vibrational state of H_2^+. Most numerical calculations have used time-dependent techniques to properly account for the (very) short pulse length of the laser field. However, multiphoton ionization rates have been obtained using time-independent complex-basis-function Floquet methods by Plummer *et al.* [9]. The work of Dundas *et al.* [6] was in very good agreement with these results. These comparisons enhance the arguments of Gavrila [10], who argued that a dual time-dependent and time-independent approach is the best technique for solving the dynamics of atoms or molecules subjected to an intense laser field.

In this paper we present a set of time-dependent calculations for the single-photon and multiphoton ionization of H_2^+ in an intense, linearly polarized, electromagnetic field. Here our focus is not on the field effects of molecules subjected to ever more intense and short-pulse laser fields (although our method can be used for such purposes), but rather to explore the single-photon and multiphoton ionization rates and cross sections resulting from a light diatomic molecule exposed to an electromagnetic field. Single-photoionization cross sections for H_2^+ in the fixed-nuclei approximation have been calculated by Bates and Öpik [11] in the 1960s for cases where the field was oriented both parallel and perpendicular to the internuclear axis, and these results have since been confirmed many times [12,13]. Plummer and McCann [13] also presented two- and three-photon ionization generalized cross sections from H_2^+ in their study of hydrogen systems, for the case where the laser field was oriented parallel to the internuclear axis. Our calculations address the full

dimensionality of the electronic coordinate while keeping the nuclear motion fixed. The system is defined in spherical coordinates centered on the center of mass of the molecule. Although the one-electron H_2^+ system is completely separable in prolate spheroidal (or confocal elliptical) coordinate systems, we choose not to take advantage of this since we plan to extend our technique to multielectron problems, which are not separable in elliptical coordinates. Our aim is to extend this method to the treatment of double photoionization of two electrons from a molecular target, i.e., the two-center, three-body Coulomb problem, by increasing the dimensions of the problem to account for two ejected electrons. The many experimental measurements of differential cross sections for double photoionization of D_2 by several groups [14–17] have not been matched by theoretical calculations for these processes. We hope that this imbalance can be addressed in the coming years. This is unlike the situation for the double photoionization of two-electron atoms, where in recent years theory and experiment have reached high levels of agreement for most dynamical situations involving the double photoionization of helium [18–20].

The structure of this paper is as follows. In the following section we show how the variational principle is used to construct the Hamiltonian for H_2^+ on a two-dimensional uniform lattice. This Hamiltonian is then diagonalized to obtain a full set of bound states of H_2^+. The time-dependent Schrödinger equation for H_2^+ is then solved and a discussion of two different time propagators used in the solution of the Schrödinger equation is given. We then present a selection of ionization cross sections obtained for H_2^+ for a variety of laser frequencies and internuclear separations of the H_2^+ ion. We conclude by discussing future directions for this work. Unless otherwise stated atomic units are used throughout this paper.

II. THEORY

Making use of the kinetic-energy functional $\frac{1}{2}\int d\vec{r}|\vec{\nabla}\psi(\vec{r},t)|^2$, a numerical representation of the time-dependent Schrödinger equation for a single electron in the field of two nuclei is derived from the variational form

$$\frac{\delta}{\delta u^*}\int_0^\infty r^2 dr \int_0^\pi \sin\theta d\theta \left(iu^*\frac{\partial u}{\partial t} - \frac{1}{2}\left|\frac{\partial u}{\partial r}\right|^2 - \frac{1}{2r^2}\left|\frac{\partial u}{\partial \theta}\right|^2 - u^* V u \right) = 0, \tag{1}$$

where the total wave function is given by

$$\psi(r,\theta,\phi,t) = \sum_m u^{(m)}(r,\theta,t)\frac{e^{im\phi}}{\sqrt{2\pi}}. \tag{2}$$

The total potential energy is given by

$$V(r,\theta,t) = V_{\text{nuclear}} + V_{\text{laser}} + V_{\text{centrifugal}}, \tag{3}$$

where the static nuclear term is

$$V_{\text{nuclear}}(r,\theta) = -\frac{Z_1}{\sqrt{r^2 + \frac{R^2}{4} - rR\cos\theta}} - \frac{Z_2}{\sqrt{r^2 + \frac{R^2}{4} + rR\cos\theta}}, \tag{4}$$

Z_1 and Z_2 are the nuclear atomic numbers, and R is the internuclear separation. The time-varying laser term is

$$V_{\text{laser}}(r,\theta,t) = E(t) f(r,\theta)\cos(\omega t), \tag{5}$$

where $E(t)$ is the electric-field amplitude, $f(r,\theta)$ defines the orientation of the field with respect to the internuclear axis, and ω is the laser frequency. The centrifugal term is

$$V_{\text{centrifugal}}(r,\theta) = \frac{m^2}{2r^2\sin^2\theta}. \tag{6}$$

If we represent the derivatives and integrals in Eq. (1) with low-order finite differences, discretizing space on a uniform mesh yields

$$i\frac{\partial w_{i,j}^{(m)}(t)}{\partial t} = (Kw)_{i,j}^{(m)}(t) + V_{i,j}(t) w_{i,j}^{(m)}(t) + E(t) r_i \cos(\theta_j)\cos(\omega t) w_{i,j}^{(m)}(t), \tag{7}$$

where the kinetic-energy operator is given by

$$(Kw)_{i,j}^{(m)}(t) = -\frac{1}{2}\left(\frac{c_i w_{i+1,j}^{(m)}(t) + c_{i-1} w_{i-1,j}^{(m)}(t) - \overline{c_i} w_{i,j}^{(m)}(t)}{\Delta r^2} \right) - \frac{1}{2r_i^2}\left(\frac{d_j w_{i,j+1}^{(m)}(t) + d_{j-1} w_{i,j-1}^{(m)}(t) - \overline{d_j} w_{i,j}^{(m)}(t)}{\Delta\theta^2} \right), \tag{8}$$

the coefficients are given by

$$c_i = \frac{r_{i+1/2}^2}{r_i r_{i+1}}, \qquad \overline{c_i} = \frac{(r_{i+1/2}^2 + r_{i-1/2}^2)}{r_i^2}, \qquad d_j = \frac{\sin\theta_{j+1/2}}{\sqrt{\sin\theta_j \sin\theta_{j+1}}}, \qquad \overline{d_j} = \frac{(\sin\theta_{j+1/2} + \sin\theta_{j-1/2})}{\sin\theta_j}, \tag{9}$$

and finally

$$w_{i,j}^{(m)}(t) = r_i\sqrt{\sin\theta_j}\, u_{i,j}^{(m)}(t). \tag{10}$$

The $V_{i,j}(t)$ terms in Eq. (7) are diagonal on the grid and are made up of the nuclear and centrifugal terms as defined above. This equation describes the case where the field is oriented parallel to the internuclear axis, i.e., $f(r,\theta) = r\cos\theta$, so that states which start with an initial symmetry m will remain with the same symmetry.

We also wish to examine single-photon and multiphoton ionization rates for the case where the laser field is oriented perpendicular to the internuclear axis. Although in strong laser fields light molecules, such as H_2^+, will quickly align parallel to the laser field direction, it is instructive to also consider the perpendicular case, which may become important for molecules subjected to weaker fields. For the case where the laser field is perpendicular to the internuclear axis, $f(r,\theta) = r\sin\theta\cos\phi$, the equations now take the form

$$i\frac{\partial w_{i,j}^{(m)}(t)}{\partial t} = (Kw)_{i,j}^{(m)}(t) + V_{i,j}(t)w_{i,j}^{(m)}(t) + \frac{1}{2}E(t)r_i\sin(\theta_j)\cos(\omega t)[w_{i,j}^{(m+1)}(t) + w_{i,j}^{(m-1)}(t)], \tag{11}$$

so that the initial m state is now coupled to states with $m \pm 1$.

A complete set of bound and continuum states for H_2^+ may be obtained by diagonalizing the Hamiltonian defined in Eqs. (7) and (11), with no laser term. In most of the calculations presented here, a distance of 40 a.u. in the radial (r) direction was used, with a mesh spacing $\Delta r = 0.1$ a.u. The θ coordinate ranged from 0 to π, and on average around 50 points were chosen with a mesh spacing $\Delta\theta = 0.02\pi$. We note that our mesh was chosen such that the positions of the two nuclei fell between two successive grid points in order to avoid a singularity on the grid. As shown in the coefficients defined in Eq. (8) a half-spacing is adopted in both coordinate directions so that our representation obeys the boundary conditions.

The center of mass of the H_2^+ molecule is chosen as the zero in our coordinate system. In Fig. 1 we show the four lowest-energy states ($1\sigma_g$, $2\sigma_u$, $2\sigma_g$, and $3\sigma_u$) of H_2^+ obtained from our diagonalization on the (r,θ) grid at the equilibrium internuclear separation of $R = 2$ a.u., for $m = 0$. These figures show only the region out to $r = 20$ a.u. even though in our calculations the full mesh out to 40 a.u. was used. The energies of these states are in excellent agreement with the exact values given by Bates *et al.* [2], to much better than 1%. The $1\sigma_g$ ground state [Fig. 1(a)] is used as the initial state in our time propagation of the Schrödinger equation (7).

Time propagation of the Schrödinger equation

Following previous time-dependent calculations of electron-impact ionization and photoionization, the time-dependent Schrödinger equation (7) can be propagated using an explicit ''leap-frog'' time propagator [21]. The time evolution of the partial differential equation (7) may be expressed as

$$w(t+\Delta t) = w(t-\Delta t) - 2i\Delta t H w(t), \tag{12}$$

which involves only one Hamiltonian matrix multiplication per time step.

This time propagator is easily implemented on massively parallel computers and norm conservation is exact if the time step is adjusted to be less than 1 divided by the eigenvalue with the largest absolute value of the discrete Hamiltonian operator. This method has proved very suitable for use in previous time-dependent calculations of electron-impact ionization and photoionization of atoms (see Ref. [22] for a review). This propagator seems particularly suited to spherically symmetric problems, such as electron and photon collisions with atoms, due to the relatively low angular-momentum expansion required to converge collision calculations. This allows a moderately sized time spacing so that a reasonable total number of time steps is used to fully converge the calculations. On the other hand, when we time propagate Eq. (7), it was found that a very small time spacing must be employed to conserve the norm and accurately propagate the time-dependent equation, mainly due to the inclusion of high angular-momentum states inherent in a discretization in the θ direction.

Due to this problem, other time propagators were tested. One which was found to be particularly suitable to this system was the implementation of an implicit time propagator. This method is based on the algorithm of Koonin [23] using a nested ordering of the r and θ terms in Eq. (7). Briefly, the Hamiltonian defined in Eq. (7) or Eq. (11) is split into its r and θ components in the form

$$w_{i,j}(t+\Delta t) = e^{-i\Delta t V_{i,j}/(t)2}\left(1+\frac{i\Delta t}{2}K_r\right)^{-1}\left(1+\frac{i\Delta t}{2}K_\theta\right)^{-1} \times\left(1-\frac{i\Delta t}{2}K_\theta\right)\left(1-\frac{i\Delta t}{2}K_r\right) \times e^{-i\Delta t V_{i,j}(t)/2}w_{i,j}(t), \tag{13}$$

where K_r is given by the first term and K_θ by the second term on the right-hand side of Eq. (8). $V_{i,j}(t)$ is composed of the nuclear, laser, and centrifugal terms defined in Eqs. (4)–(6). This solution has been implemented on a massively parallel computer, but the matrix inversion steps are much slower than the matrix multiplication steps.

On a massively parallel computer, for the same time step Δt, the explicit propagator of Eq. (12) is much faster than the implicit propagator of Eq. (13). However, much larger time steps may be employed using the implicit propagator, as opposed to using the explicit propagator. For the molecular problem on a discretized mesh in both r and θ, we found that the larger time steps offset the slower parallel algorithm and that the implicit propagator is faster and more efficient than the explicit propagator. All the calculations presented in the paper were made using the implicit propagator. We make two cautionary notes. First, for other numerical problems on mas-

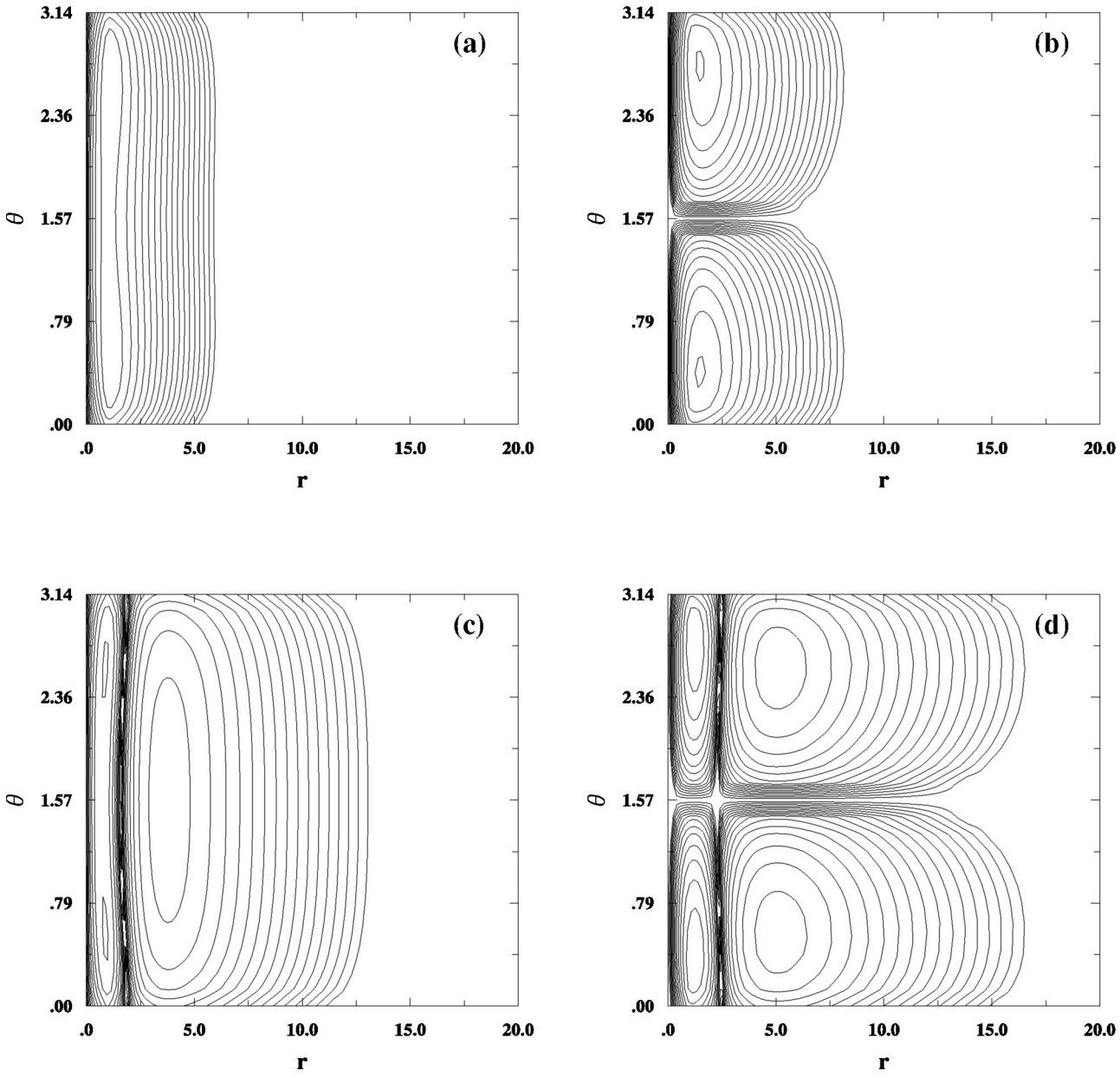

FIG. 1. Four lowest σ wave functions of the H_2^+ molecule obtained by diagonalization of the Hamiltonian: (a) $1s\sigma_g$ state, (b) $2p\sigma_u$ state, (c) $2s\sigma_g$ state, and (d) $3p\sigma_u$ state. In this case the radial coordinate r extends to 20 a.u with a mesh spacing of 0.1 a.u. Twenty-five points with a mesh spacing of 0.04π were used in the θ coordinate.

sively parallel machines, one may find the explicit propagator to be faster and more efficient than the implicit propagator. Second, whereas the explicit propagator fails dramatically when the time step is too large, the error in the implicit propagator grows slowly with increasing time step and must be carefully monitored for accurate results.

The Schrödinger equation (7) was time propagated for between 15 and 20 field periods. Several pulse shapes were examined; in order to better define a cross section, a pulse shape was chosen that turned on and off over one period, and was constant for between 10 and 15 periods. The wave function was then propagated for several more periods before interrogation. Most of our calculations were made at field intensities of between 10^{13} and 10^{14} W cm^{-2}.

After time propagation the time-dependent wave function was projected onto the complete set of bound states of H_2^+ obtained from the diagonalization of the Hamiltonian. The probability for ionization is then given by

$$\mathcal{P}=1-\sum_{lm}\int dr\int d\theta|\psi(r,\theta,t)|\phi_{lm}(r,\theta)|^2, \qquad (14)$$

where $\phi_{lm}(r,\theta)$ are the bound states of H_2^+. The (n-photon) ionization cross section is then given by

$$\sigma_n=\left(\frac{\omega}{I}\right)^n\frac{\mathcal{P}}{T}, \qquad (15)$$

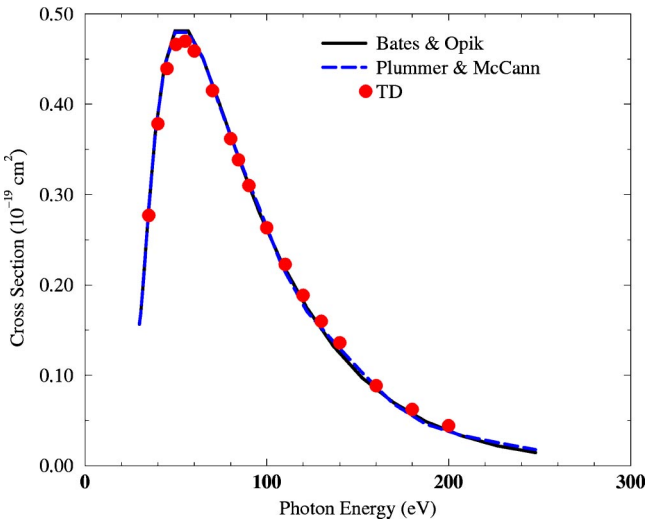

FIG. 2. Single-photoionization cross sections for H_2^+ as a function of photon energy for the case where the laser field is oriented parallel to the internuclear axis. The time-dependent results (circles) are compared with those of Bates and Öpik [11] (solid line) as well as the results of Plummer and McCann [13] (long-dashed line).

where $\mathcal{T}$ is the integral of the laser-pulse shape with respect to time. The units of these cross sections are then cm^{2n} s^{n-1}.

III. RESULTS

A. Single photoionization

As a check on our method, we first calculated the single-photoionization cross section of H_2^+ as a function of incident-photon energy, for the case where the laser field is oriented parallel to the internuclear axis. Our results are shown in Fig. 2. Here we have the essentially "exact" results of Bates and Öpik [11] to compare with. We also compare with the Floquet results of Plummer and McCann [13]. The time-dependent results, given by the circles, are in excellent agreement with the results of Bates and Öpik as well as the Floquet results. Our results are only very weakly dependent on intensity, with a difference of at most 5% at the highest frequencies considered. We also checked that our results did not depend strongly on the length of pulse chosen, or the way in which the pulse was turned on or off. Calculations in which the pulse was turned on and off over six laser cycles and kept at a constant value for eight total cycles were in very good agreement with the results presented here, with only a slight difference in cross section near the peak.

The time evolution of the initial wave function is shown in Fig. 3 for photoionization with a 45 eV photon. At the initial time $t=0.0$ the wave function starts in the $1\sigma_g$ ground state. After propagation of the time-dependent Schrödinger equation, and after the wave function has "settled down," at $t=57.0$ a.u., it is clear that most of the wave function has remained in the $1\sigma_g$ ground state. However, there is clearly some continuum σ_u character to the wave function at larger radial distances, which is a signal of photoionization into $\epsilon\sigma_u$ continuum states. The characteristic node of a σ_u wave function, around $\pi/2$, demonstrated in Fig. 1(b), is clearly evident in the wave-function region in Fig. 3(b) at large radial distances.

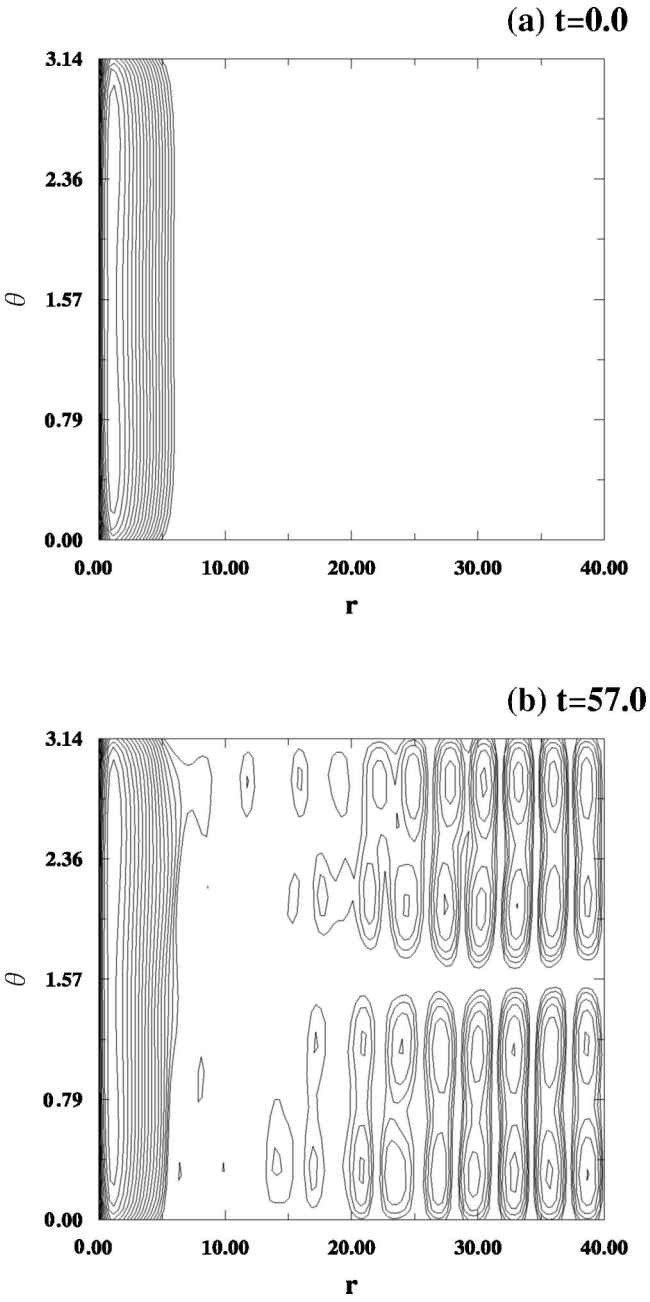

FIG. 3. Time-dependent wave function for H_2^+, (a) before and (b) after photoionization with a 45 eV incident photon, for the case where the field is oriented parallel to the internuclear axis. All distance and time quantities are in atomic units.

In Fig. 4 we show our results for single photoionization of H_2^+ for the case where the laser field is oriented perpendicular to the internuclear axis. Although in strong fields light molecules such as H_2^+ will align quickly with the orientation of the field, in weaker fields, where we also wish to apply our method, photoionization from this path may become important. The total photoionization cross section, calculated by averaging over all orientations, is also dominated by this path, which in this case will involve a transition to the π_u state of H_2^+. Again we are able to compare with the results of Bates and Öpik [11] for this perpendicular case. It is clear that the time-dependent results, shown by the circles,

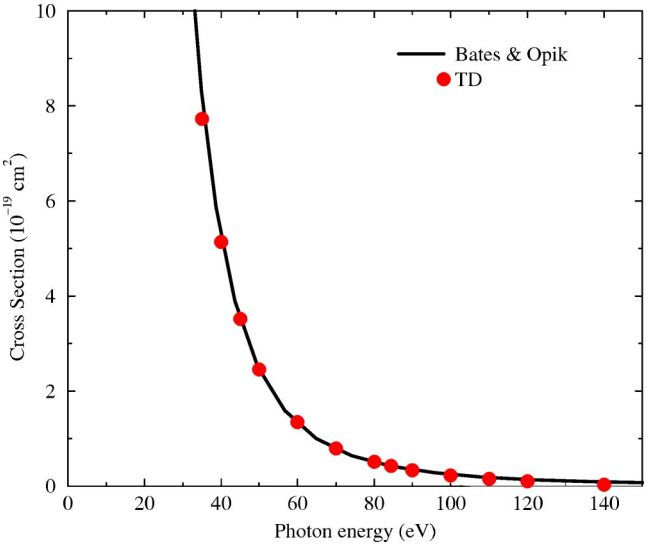

FIG. 4. Single-photoionization cross sections for H_2^+ as a function of photon energy for the case where the laser field is oriented perpendicular to the internuclear axis. The time-dependent results (circles) are compared with those of Bates and Öpik [11] (solid line).

are again in excellent agreement with the effectively exact calculations of Bates and Öpik. We note that the photoionization cross section in this case is around an order of magnitude larger than the previous parallel orientation case, and so will become important in photoionization by less intense electromagnetic fields that do not quickly align the molecules.

Figure 5 shows the final wave function in the (a) $1\sigma_g$ ground state and (b) $\epsilon\pi_u$ continuum state after photoionization with a 40-eV photon. We note that the wave function plot shown in Fig. 5(b) is renormalized. The magnitude of the contours in Fig. 5(b) are much less than those in Fig. 5(a) reflecting the fact that most of the wave function has remained in the initial $1\sigma_g$ state.

B. Two-photon ionization

We now turn to calculations of multiphoton ionization cross sections for H_2^+. Here we can also compare with the Floquet calculations of Plummer and McCann [13]. They examined two-photon cross sections for various values of the internuclear separations at field intensities ranging from 1.76×10^{11} to 1.76×10^{14} W cm^{-2}, for the case where the laser field is oriented parallel to the internuclear axis. In general, their results showed ionization cross sections dominated by resonances caused by one-photon transitions between the ground $1\sigma_g$ state and successive σ_u states which converge to the single-ionization threshold around 30 eV (1.1026 a.u.). Our time-dependent calculations do not map these resonances since the time scale of our calculations are very much shorter than the time associated with the resonance widths. However, it is still instructive to compare calculations since the time-dependent results should give a reasonable estimate of the direct two-photon background ionization cross section.

In Fig. 6 we present the two-photon ionization cross section for H_2^+ for two internuclear separations, (a) the equilibrium separation of $R=2$ and (b) $R=6$ a.u., for the case where the laser field is oriented parallel to the internuclear axis. We compare the Floquet results calculated at 1.76×10^{13} [13] with time-dependent calculations made at intensities of 1.76×10^{13} and 1.76×10^{14} W cm^{-2}. Our results are presented as "generalized" cross sections, with units of cm^4 W^{-1}, for closer comparison with the Floquet

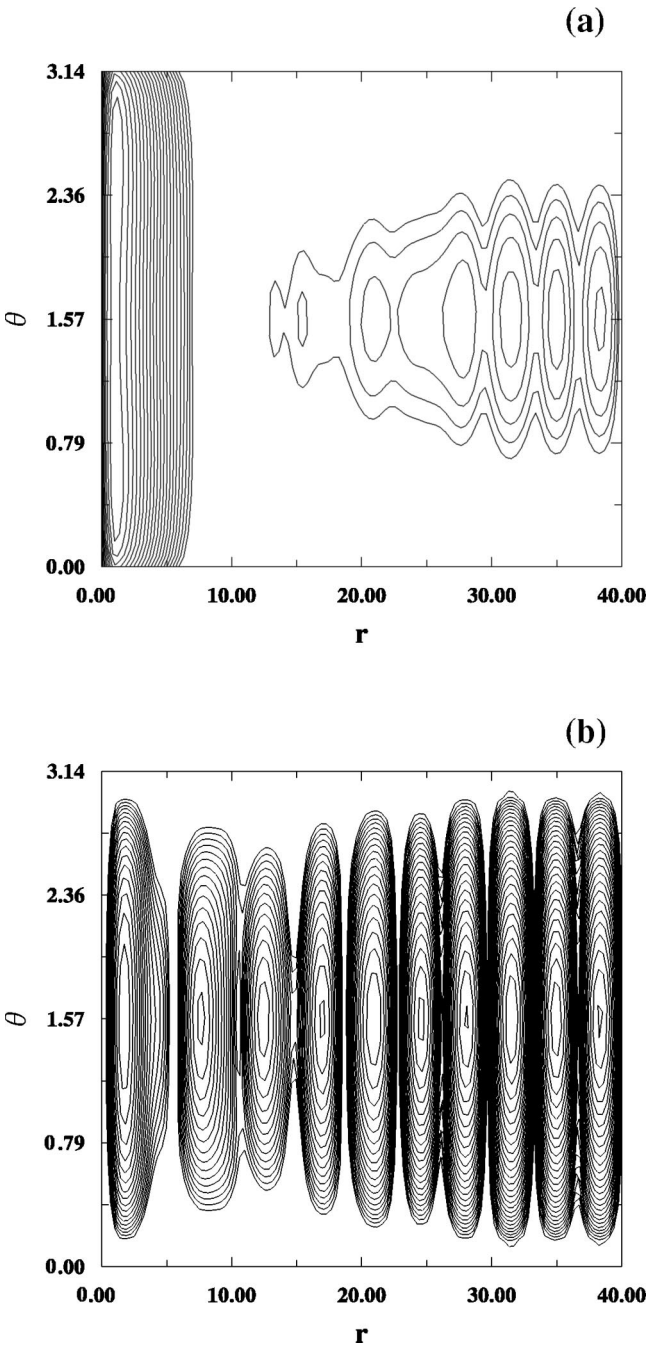

FIG. 5. Time-dependent wave function for H_2^+ after photoionization with a 40 eV incident photon, for the case where the field is oriented perpendicular to the internuclear axis. The wave function initially starts in a $1s\sigma_g$ state [shown in Fig. 3(a)]. In this figure (a) shows the $1s\sigma_g$ state after time propagation of the Schrödinger equation and (b) shows the $\epsilon\pi_u$ state, which initially starts at zero. All distance quantities are in atomic units.

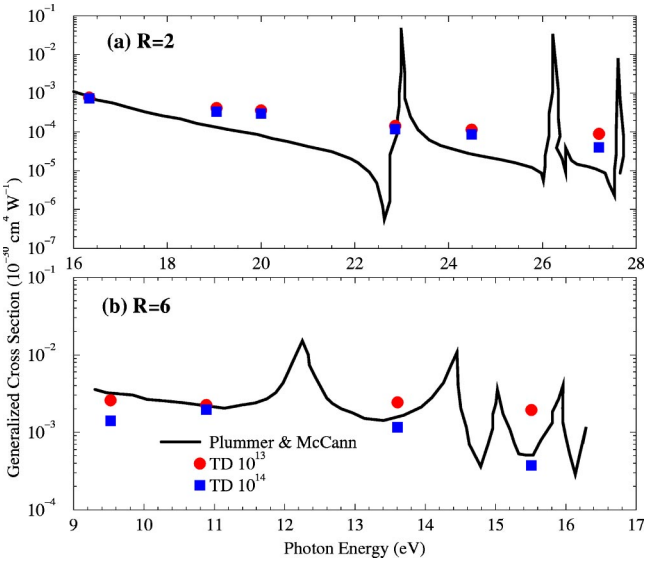

FIG. 6. Two-photon ionization cross sections for H_2^+ as a function of photon energy for the case where the laser field is oriented parallel to the internuclear axis, for two values of the internuclear separation, (a) $R=2.0$ a.u and (b) $R=6.0$ a.u. The time-dependent results at two intensities of 1.76×10^{13} (circles) and 1.76×10^{14} (squares) W cm^{-2} are compared with those of Plummer and McCann [13] (solid line).

results. These are different from our usual units defined by Eq. (15), of cm^4 s for two-photon ionization. For the $R=6$ case the ionization threshold is of course lower than that from the equilibrium separation; our diagonalization results in a threshold of 18.55 eV, which is again in very good agreement with the value given by Bates *et al.* [2]. This means that the threshold for two-photon ionization is lower for the $R=6$ case than for the $R=2$ case. We focus here on the regions between the two-photon and one-photon threshold where two-photon ionization dominates.

In general, the two-photon ionization cross sections are in very good agreement with the Floquet results for both internuclear separations. As already discussed, the time-dependent calculations do not map out the resonances shown in the Floquet work, but are in good agreement with the background (direct) ionization cross section. We note that, especially for the case where $R=6$ a.u., some intensity dependence of our ionization cross sections is seen, with the higher intensity calculations at 1.76×10^{14} W cm^{-2} somewhat lower than the 1.76×10^{13} W cm^{-2} calculations at certain photon energies. We comment that at the lowest intensities used in the Floquet calculations (1.76×10^{11} W cm^{-2}) our time-dependent calculations can become numerically unstable due to the very low probabilities for ionization.

In Table I we present the two-photon ionization cross sections for H_2^+ for cases where the laser field is oriented both parallel and perpendicular to the internuclear axis, for the case where the internuclear separation is $R=2$ a.u. Table II shows similar results for the case where $R=6$ a.u. We tabulate our results in two-photon cross section units of cm^4 s to be consistent with our previous time-dependent calculations. As in Fig. 6 we show cross sections at two laser intensities, 1.76×10^{13} and 1.76×10^{14} W cm^{-2}. It is interesting to note that our results for the perpendicular orientation case appear to be more sensitive to intensity than the parallel orientation case.

TABLE I. Two-photon ionization cross sections in cm^4 s for $R=2.0$ a.u. for cases where the laser field is oriented both parallel and perpendicular to the internuclear axis. The cross sections, in units of cm^4 s, are shown for two laser intensities, given in W cm^{-2}. The numbers in brackets following the cross section show the power of ten by which the cross section is multiplied.

	Parallel		Perpendicular	
ω (eV)	1.76×10^{13}	1.76×10^{14}	1.76×10^{13}	1.76×10^{14}
16.3	2.0 [−51]	1.9 [−51]	4.1 [−51]	2.9 [−51]
20.0	1.2 [−51]	9.5 [−52]	1.8 [−51]	1.0 [−51]
24.5	4.5 [−52]	3.4 [−52]	2.2 [−51]	3.8 [−52]
27.2	3.9 [−52]	1.8 [−52]	7.0 [−51]	7.5 [−52]

C. Three-photon ionization

We now turn to comparisons of our three-photon ionization cross sections with those of Plummer and McCann [13] made at an intensity of 1.76×10^{13} W cm^{-2}. For the equilibrium internuclear separation of $R=2$ a.u., three-photon ionization can occur above 10 eV and dominates in the photon energy range from 10 to around 15 eV, before the two-photon ionization threshold. For the case where the internuclear separation is $R=6$ a.u. the three-photon region is from around 6.2 eV to around 9 eV.

In Fig. 7(a) our time-dependent results are shown, again for two field intensities of 1.76×10^{13} and 1.76×10^{14} W cm^{-2}, in generalized cross section units of cm^6 W^{-2}, to facilitate comparison. The Floquet results (solid line) includes a broad resonance around 12 eV associated with a one-photon transition between the ground state and the lowest σ_u state. The subsequent resonances in Fig. 7(a) are associated with two-photon transitions to excited σ_g states. The very broad width of the first resonance in Fig. 7(a) distorts the comparisons with the time-dependent results. However the trend in the background (direct) three-photon ionization cross section appears in good agreement with the time-dependent results. We note also that the time-dependent cross sections calculated at 1.76×10^{13} W cm^{-2}

TABLE II. Two-photon ionization cross sections in cm^4 s for $R=6.0$ a.u. for cases where the laser field is oriented both parallel and perpendicular to the internuclear axis. The cross sections, in units of cm^4 s, are shown for two laser intensities, given in W cm^{-2}. The numbers in brackets following the cross section show the power of ten by which the cross section is multiplied.

	Parallel		Perpendicular	
ω (eV)	1.76×10^{13}	1.76×10^{14}	1.76×10^{13}	1.76×10^{14}
9.5	4.0 [−51]	2.1 [−51]	8.4 [−51]	1.6 [−51]
10.9	3.9 [−51]	3.4 [−51]	3.0 [−50]	3.5 [−51]
13.6	5.3 [−51]	2.5 [−51]	9.3 [−51]	6.3 [−52]
15.5	4.8 [−51]	9.3 [−52]	2.9 [−51]	5.1 [−52]

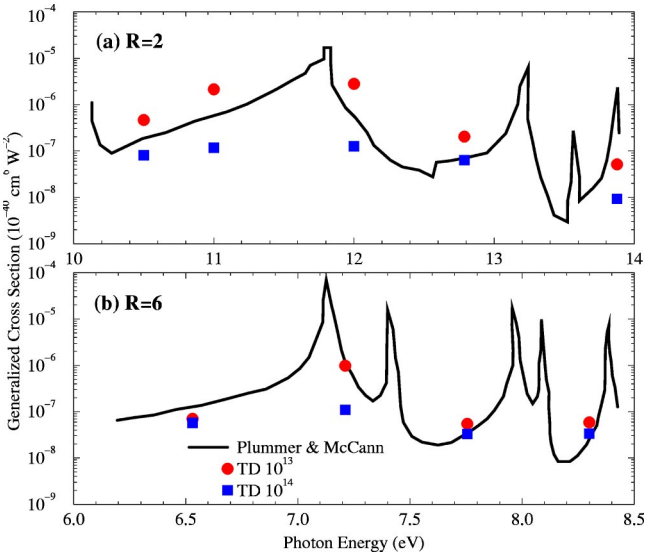

FIG. 7. Three-photon ionization cross sections for H_2^+ as a function of photon energy for the case where the laser field is oriented parallel to the internuclear axis, for two values of the internuclear separation, (a) $R=2.0$ a.u and (b) $R=6.0$ a.u. The time-dependent results at two intensities of 1.76×10^{13} (circles) and 1.76×10^{14} (squares) W cm^{-2} are compared with those of Plummer and McCann [13] (solid line).

are consistently larger than the higher intensity calculations. This difference between the time-dependent calculations at different intensities is not seen in the calculations for $R=6$ a.u., except at one-photon energy. We comment that, for these three-photon cross sections, the generalized ionization cross section appears to show more intensity dependence, which is a sign that we are leaving the perturbative regime. For higher-photon transitions the definition of a cross section may become untenable since the cross section can depend more strongly on the pulse shape and intensity.

For the $R=6$ a.u. case, the time-dependent results are generally in good agreement with the Floquet results. At this internuclear separation all the resonances in the Floquet calculations arise from two-photon transitions, which have a much smaller width than the large resonance associated with the one-photon transition in the $R=2$ a.u. results. This allows a more straightforward comparison of the time-dependent calculations with the background or direct three-photon ionization cross section.

IV. SUMMARY

In this paper we have set out a time-dependent technique to study the single-photon and multiphoton ionization of the one-electron H_2^+ molecule. We have chosen here to focus on one-, two-, and three-photon ionization cross sections, unlike previous time-dependent calculations which routinely examine many-photon transitions. For larger multiphoton ionization processes a cross section can be much harder to define, and generally ionization rates, rather than cross sections, are presented for these cases. We limit ourselves here to low-photon transitions in order to more easily define an ionization cross section.

Our single-photon ionization cross sections are in excellent agreement with exact calculations of Bates and Öpik [11] for the cases where the field is oriented both parallel and perpendicular to the internuclear axis. For the parallel case, our results are also in excellent agreement with results made using Floquet techniques made by Plummer and McCann [13].

We have also compared results for two- and three-photon ionization with the Floquet results. In general, the agreement between the multiphoton ionization cross sections calculated by the Floquet method and by our time-dependent method is good. Comparisons are hard to make with time-independent calculations such as the Floquet technique, due to the rich resonant structure observed from intermediate one- or two-photon transitions. As discussed earlier, the short time scales of the current time-dependent calculations do not allow sufficient times for these resonances to develop in the current calculations. Time-dependent calculations have however, been made which explicitly ''map out'' the formation of resonances [24] for the case of an autoionizing state formed by dielectronic capture in helium and also for autoionizing states formed by above-threshold-ionization [25]. To date, no time-dependent calculations have been made which map out bound-state resonant structures in H_2^+ such as detailed earlier. Our time-dependent method could, in principle, be extended to map out the resonances in the current problem, but this would be a large calculation in its own right. Here we concentrate only on the direct n-photon ionization. However, these fixed-nuclei time-dependent calculations are an important first step before inclusion of the nuclear motion into the solution.

In future work, we aim to go beyond the Born-Oppenheimer approximation by including the nuclear motion into the problem rather than mapping our resonances in the current problem, since any resonant structure will be modified and possibly 'washed away' by the vibrational motion of the H_2^+ molecule, especially for the larger internuclear separation calculations. This will allow a whole class of phenomena to be studied such as vibrational excitation and the Coulomb explosion. Our main aim is the time-dependent description of single and double photoionization of the two-electron H_2 molecule, work which we hope will address the imbalance between theory and experiment which exists for two-electron ejection from molecular targets. This extension of our method will require significant computational resources to describe the coupled motion of two electrons by two coordinates for each electron. Work on this is in progress.

ACKNOWLEDGMENTS

This work was supported in part by the National Science Foundation, a DOE grant (Grant No. DE-FG05-99ER5438), and a DOE SciDAC grant (Grant No. DE-FG02-01ER54G44) to Auburn University. Computational work was performed at the National Energy Research Scientific Computing Center (NERSC) at Oakland, CA.

[1] *Molecules in Intense Laser Fields*, edited by A.D. Bandrauk (Marcel Dekker, New York, 1993).
[2] D.R. Bates, K. Ledsham, and A.L. Stewart, Proc. R. Soc. London Ser. A **246**, 28 (1953).
[3] T. Zuo, S. Chelkowski, and A.D. Bandrauk, Phys. Rev. A **49**, 3943 (1994).
[4] S. Chelkowski, C. Foisy, and A.D. Bandrauk, Phys. Rev. A **57**, 1176 (1998).
[5] A.D. Bandrauk and N.H. Shon, Phys. Rev. A **66**, 031401(R) (2002).
[6] D. Dundas, J.F. McCann, J.S. Parker, and K.T. Taylor, J. Phys. B **33**, 3261 (2000); D. Dundas, Phys. Rev. A **65**, 023408 (2002).
[7] G.L. Ver Steeg, K. Bartschat, and I. Bray, J. Phys. B **36**, 3325 (2003).
[8] B. Feuerstein and U. Thumm, Phys. Rev. A **67**, 043405 (2003).
[9] M. Plummer, J.F. McCann, and L.B. Madsen, Comput. Phys. Commun. **114**, 94 (1998); L.B. Madsen, M. Plummer, and J.F. McCann, Phys. Rev. A **58**, 456 (1998).
[10] M. Gavrila, in *Photon and Electron Collisions with Atoms and Molecules*, edited by P.G. Burke and C.J. Joachain (Plenum Press, New York, 1997), p. 147.
[11] D.R. Bates and U. Öpik, J. Phys. B **1**, 543 (1968).
[12] J.A. Richards and F.P. Larkin, J. Phys. B **19**, 1945 (1986).
[13] M. Plummer and J.F. McCann, J. Phys. B **28**, 4073 (1995).
[14] T.J. Reddish, J.P. Wightman, M.A. MacDonald, and S. Cvejanović, Phys. Rev. Lett. **79**, 2438 (1997).
[15] J.P. Wightman, S. Cvejanović, and T.J. Reddish, J. Phys. B **31**, 1753 (1998).
[16] R. Dörner, H. Bräuning, O. Jagutzki, V. Mergel, M. Achler, R. Moshammer, J.M. Feagin, T. Osipov, A. Bräuning-Demian, L. Spielberger, J.H. McGuire, M.H. Prior, N. Berrah, J.D. Bozek, C.L. Cocke, and H. Schmidt-Böcking, Phys. Rev. Lett. **81**, 5776 (1998).
[17] D.P. Seccombe, S.A. Collins, T.J. Reddish, P. Selles, L. Malegat, A.K. Kazansky, and A. Huetz, J. Phys. B **35**, 3767 (2002).
[18] J. Colgan, M.S. Pindzola, and F. Robicheaux, J. Phys. B **34**, L457 (2001).
[19] P. Selles, L. Malegat, and A.K. Kazansky, Phys. Rev. A **65**, 032711 (2002).
[20] G. Turri, L. Avaldi, P. Bolognesi, R. Camilloni, M. Coreno, J. Berakdar, A.S. Kheifets, and G. Stefani, Phys. Rev. A **65**, 034702 (2002).
[21] W.H. Press, S.A. Teukolsky, W.T. Vetterling, and B.P. Flannery, *Numerical Recipes* (Cambridge University Press, New York, 1992), p. 833.
[22] M.S. Pindzola, F. Robicheaux, J. Colgan, D.M. Mitnik, D.C. Griffin, and D.R. Schultz, in *Photonic, Electronic, and Atomic Collisions: ICPEAC XXII*, edited by J. Burgdörfer, J.S. Cohen, S. Datz, and C.R. Vane (Rinton Press, New Jersey, 2002), p. 483.
[23] S.E. Koonin and D.C. Meredith, *Computational Physics* (Addison-Wesley, New York, 1990), p. 174.
[24] D.M. Mitnik, D.C. Griffin, and M.S. Pindzola, Phys. Rev. Lett. **88**, 173004 (2002).
[25] J.S. Parker, L.R. Moore, K.J. Meharg, D. Dundas, and K.T. Taylor, J. Phys. B **34**, L69 (2001).